Memoirs of the Faculty of Engineering, Okayama University, Vol.24, No. 1, November 1989

Propagation Characteristics of Superlattice Potentials and their Optimization

Hiroo Totsuji* and Teruki Hatatani*

(Received October 16 , 1989)

SYNOPSIS

Propagation of charged carriers in semiconductor superlattices is analyzed on the basis of the effective mass approximation with appropriate boundary conditions at heterojunctions taken into account. Applying the finite element method, clarified are the effects of details of the potential profile, such as linear and smooth gradings and random fluctuations, on characteristics of superlattices which are expected to work as collector barriers and energy filters in electronic devices.

1. Introduction

Owing to recent developments in technologies of crystal growth such as molecular beam epitaxy (MBE) and metalorganic chemical vapor deposition (MOCVD), we are now able to create a tailored potential profile, or superlattice potentials,[1] for electrons or holes in compound semiconductors. These structures are now going to be utilized to control flow of carriers in various electronic devices.[2-4]

In order to achieve desired functions in such devices, it is necessary to know how to optimize the propagation of electrons or holes with respect to the profiles of the potentials. The purpose of this paper is to describe some preliminary results on the effects of shapes of superlattice potentials on the static propagation characteristics of carriers which have been obtained by applying a numerical method.

In what follows we restrict ourselves within the one-dimensional case and consider only the most simple and well known superlattices of GaAs and AlGaAs.

*Department of Electrical and Electronic Engineering

2. Method of Analyses

When the effect of abrupt change of the potential at the interfaces (heterojunctions) of different materials is taken into account by the transfer matrix, the propagation of charges in superlattice potentials may be determined by the Schrödinger equation for the envelope function in the effective mass approximation.[5] We have thus

$$\left[-\frac{\hbar^2}{2m^*}\frac{d^2}{dz^2} + V(z) \right]\psi(z) = E\psi(z), \tag{2.1}$$

where m^* is the effective mass. The boundary condition at a heterointerfaces at $z=z_0$ is generally given by the transfer matrix T

$$\begin{pmatrix} \psi \\ a\dfrac{d\psi}{dz} \end{pmatrix}_{z=z_0+0} = T \begin{pmatrix} \psi \\ a\dfrac{d\psi}{dz} \end{pmatrix}_{z=z_0-0}, \tag{2.2}$$

where a is the lattice constant.

In superlattices composed of GaAs and $Al_xGa_{1-x}As$, the potential V(x), the effective mass $m^*(x)$, and the transfer matrix are approximately given respectively by[6]

$$V(x) - V(x=0) = 0.8x \ [eV], \tag{2.3}$$

$$m^*/m_0 = 0.067 + 0.083x, \tag{2.4}$$

$$T = \begin{pmatrix} 1 & 0 \\ 0 & \dfrac{m(x(z_0+0))}{m(x(z_0-0))} \end{pmatrix}, \tag{2.5}$$

where m_0 is the electronic mass. When we adopt (2.5) as the transfer matrix, eq.(2.1) with (2.2) is expressed in the form

$$\left[-\frac{\hbar^2}{2}\frac{d}{dt}\frac{1}{m^*(z)}\frac{d}{dz} + V(z) \right]\psi(z) = E\psi(z). \tag{2.6}$$

Here the potential V and the effective mass m^* are regarded as functions of position with step discontinuities and the zero of the potential is taken in the GaAs domain.

The above equation may also be derived when the composition of

materials is gradually changing: The latter case can be regarded as a collection of infinitely short steps with constant composition. We may thus study the propagation of carriers in superlattices composed of GaAs-$Al_xGa_{1-x}As$ based on eq. (2.6).

The analyses of this kind of equations have already been performed by dividing the space into segments: Either the potential is regarded as constant or linear function of distance in each segment[7] or the finite element method (FEM) is employed.[8]

In order to make a computation in cases of arbitrary potential profiles, the FEM may be the most useful method. In FEM, the solution of the original equation in each segment is expressed by a finite number of basis functions $\{\phi_i\}$ as

$$\psi = \sum_i a_i \phi_i, \tag{2.7}$$

Here the coefficients are directly related to the values of the wave function and its derivatives at the end points of segments. Determining the coefficients by the Galerkin method, we have for the element (z_1, z_2)

$$\sum K_{ij} \phi_j = E \sum M_{ij} \phi_j, \tag{2.8}$$

$$K_{ij} = \frac{\hbar^2}{2} \int_{z_1}^{z_2} \frac{d\phi_i}{dz} \frac{1}{m^*(z)} \frac{d\phi_j}{dz} dz - \frac{\hbar^2}{2} \left[\phi_i \frac{1}{m^*(z)} \frac{d\phi_j}{dz} \right]_{z_1}^{z_2} + \int_{z_1}^{z_2} \phi_i V(z) \phi_j dz, \tag{2.9}$$

$$M_{ij} = \int_{z_1}^{z_2} \phi_i \phi_j dz. \tag{2.10}$$

The boundary conditions at the interfaces are given by (2.5).

The equation for the whole system is obtained by combining the one for each element. The resultant equation for the coefficients is solved as a boundary value problem; with the boundary condition at x=L, L being a large positive value,

$$\psi(z=L) = \exp(ikL) \tag{2.11}$$

the solution is computed and the values at the other boundary is used to determine the transmission and reflection coefficients, T and R, as

$$T^{-1} = \frac{1}{4} \left| \psi(-L) + \frac{1}{ik} \frac{d}{dz} \psi(-L) \right|^2, \tag{2.12}$$

$$R = 1 - T. \tag{2.13}$$

The number of elements is determined by confirming the convergence of the result and is less than 200 in most cases.

3. Examples

(a) Collector barrier

In order to support an appropriate potential difference between the base and the collector and to allow only the carriers with higher energies into the collector, a potential barrier is sometimes placed between these two electrodes.[2,3] In this case, we need classical propagation characteristics, i.e. sharpness of the transition from opaque to transparent barrier and smallness of the interference effect in the transparent domain as a function of the incident energy.

To have a sharp transition, relatively thick barriers are used, and to reduce the reflection at the entrance of the barrier, the graded profile is often adopted instead of potential steps.

As an example, we here consider a barrier of thickness 500Å with the height 0.16eV. The transmission coefficient of such a potential step is plotted in Fig.1a as a function of incident energy. Since changes within thermal energy may be irrelevant, averaged values over k_BT (T=300K) are also plotted in Fig.1b.

The effect of linear grading is shown by some examples in Figs.2a-2f: Here only averaged values are plotted. We first observe that the grading at the exit has the same effect on the transmission coefficient: The effect of interference between waves in opposite directions is suppressed by the grading both at the entrance and the exit of the barrier. Though being simply a result of the fact that the scattering matrix is unitary, this fact may be worth noting in designing some devices.

In order to have a classical characteristics, gradings with larger width at both ends are helpful. The increase of the width over 50Å, however, is not so effective: This is consistent with the fact that the wavelength for 0.16eV before entering the barrier is 118Å.

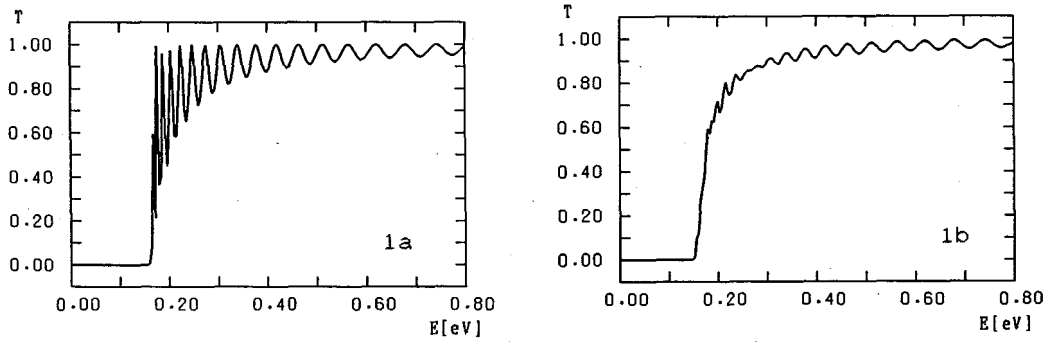

Figs.1a and 1b. Transmission coefficient T of a potential step of width 500Å and height 0.16eV ($Al_{0.2}Ga_{0.8}As$) (a) and values averaged over thermal energy k_BT at T=300K (b).

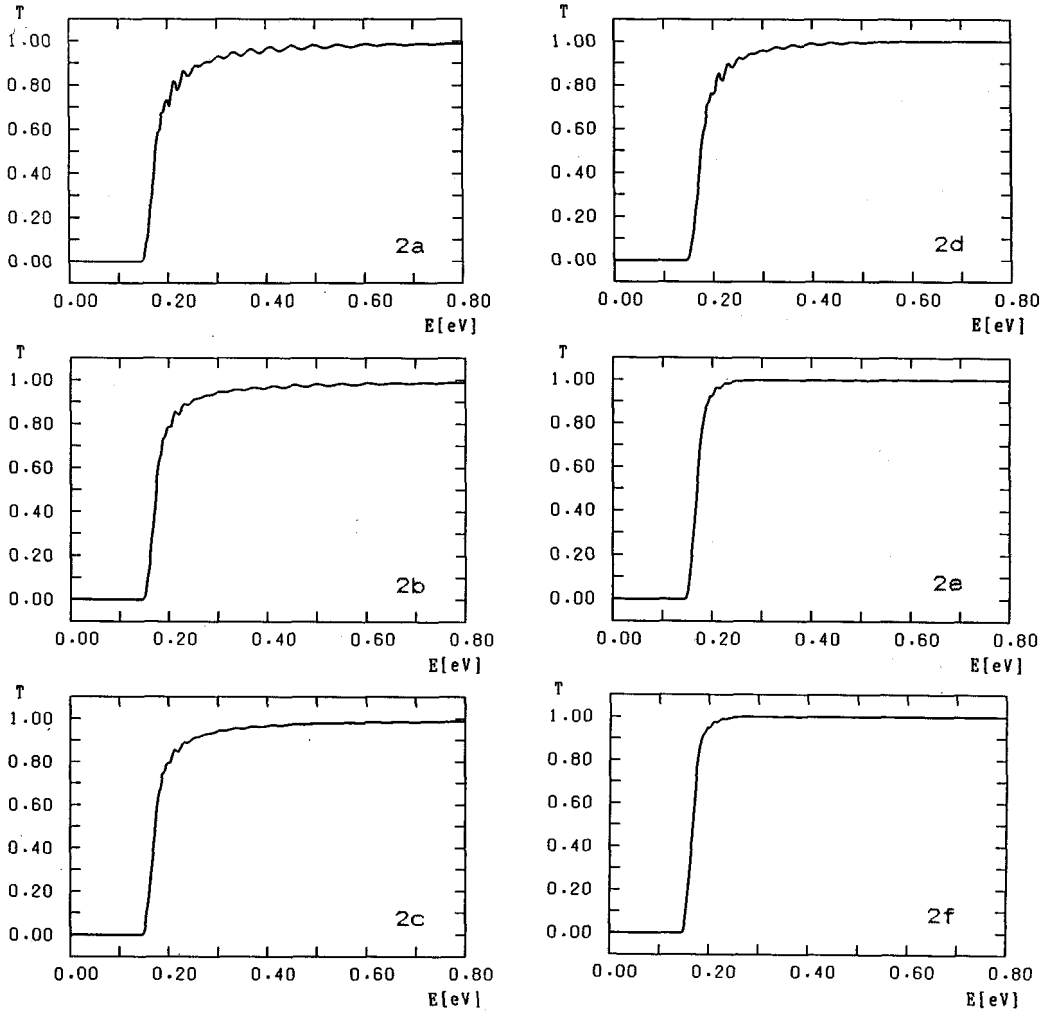

Figs.2a-2f. Effect of linear gradings at one side (a, b, c) and at both sides (d, e, f) of width 25Å(a, d), 50Å(b, e), and 100Å(c, f). Values of T averaged over thermal energy are shown.

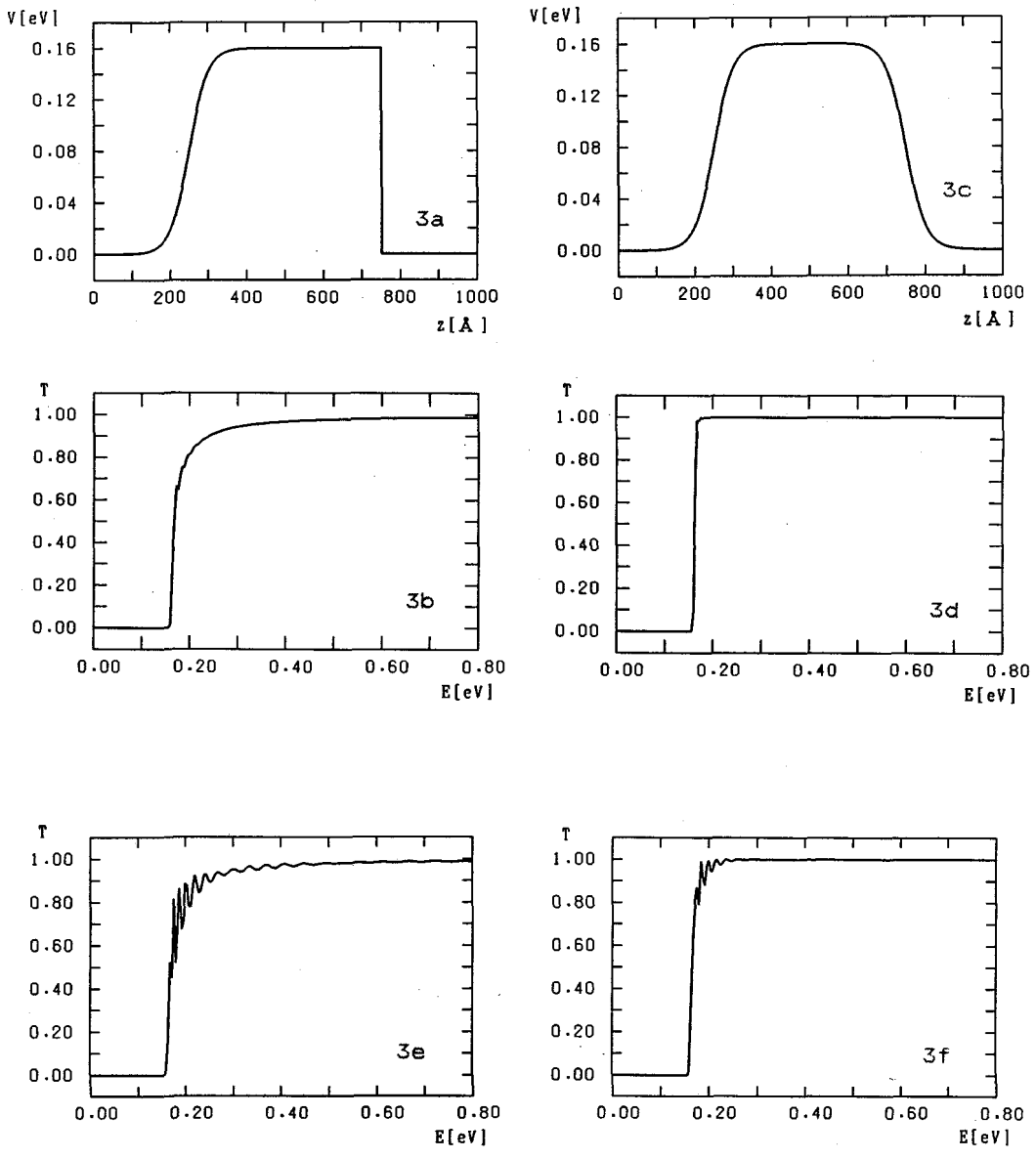

Figs.3a-3f. Effect of smooth gradings at one (a, b) and both (c, d) sides. Values without thermal average are plotted; those of the case of linear gradings at one (e) and both (f) sides are also shown.

Examples of smooth gradings are shown in Fig.3a and 3b in comparison with the linear grading of the width 100Å at one and both ends shown in Fig.3c and 3d. Here the functional form tanh is adopted and the gradient at the center of grading is adjusted to be the same as in the case of linear grading of 100Å. In these figures, values *without* averaging over thermal energy are plotted. We see that smooth gradings are very effective to have classical transmission especially in the case of gradings at both ends where we have almost classical characteristics. In the case of grading at one end, smoothness reduces the oscillations drastically.

(b) Energy filters

When potential wells are coupled by relatively thin barriers, the quasi-levels form a band of allowed energy states. For electrons also with energies larger than the height of barriers, quantum interference gives a structure and these arrays of barriers and wells have been proposed as a kind of energy filter for charge carriers.[4]

The structure of the band of transmission is determined by the width of constituent wells and the thickness of barriers between them. In principle, the former determines the position of resonance levels and the latter the band width. The characteristics of these filters, however, are difficult to predict without making computations for each case. Here we analyze to what extent the details of the potential profiles affect the transmission coefficient.

An example of the change of the transmission coefficient with the structure of the filter is shown in Fig.4a. The ratio of the widths of adjacent well and barrier (of height 0.16eV) is changed from 1:9 to 9:1, their sum being fixed to be 100Å.

The behavior of the lower three bands may be interpreted as the lowering of eigenenergy with increase of the width of the well. The behavior of the transmission coefficient between allowed bands, especially for higher bands, does not seem to allow simple interpretations.

The effect of the detailed potential profile is shown in Fig.4b where the barriers in the case of well-barrier ratio 6:4 are modified into sinusoidal forms. We observe that the change of the profile largely affect the transmission for carriers with energies higher than barriers and has a tendency to eliminate interference effects. This tendency is consistent with the fact that the corresponding wavelength is nearly equal to the width of well which is not well defined for sinusoidal barriers.

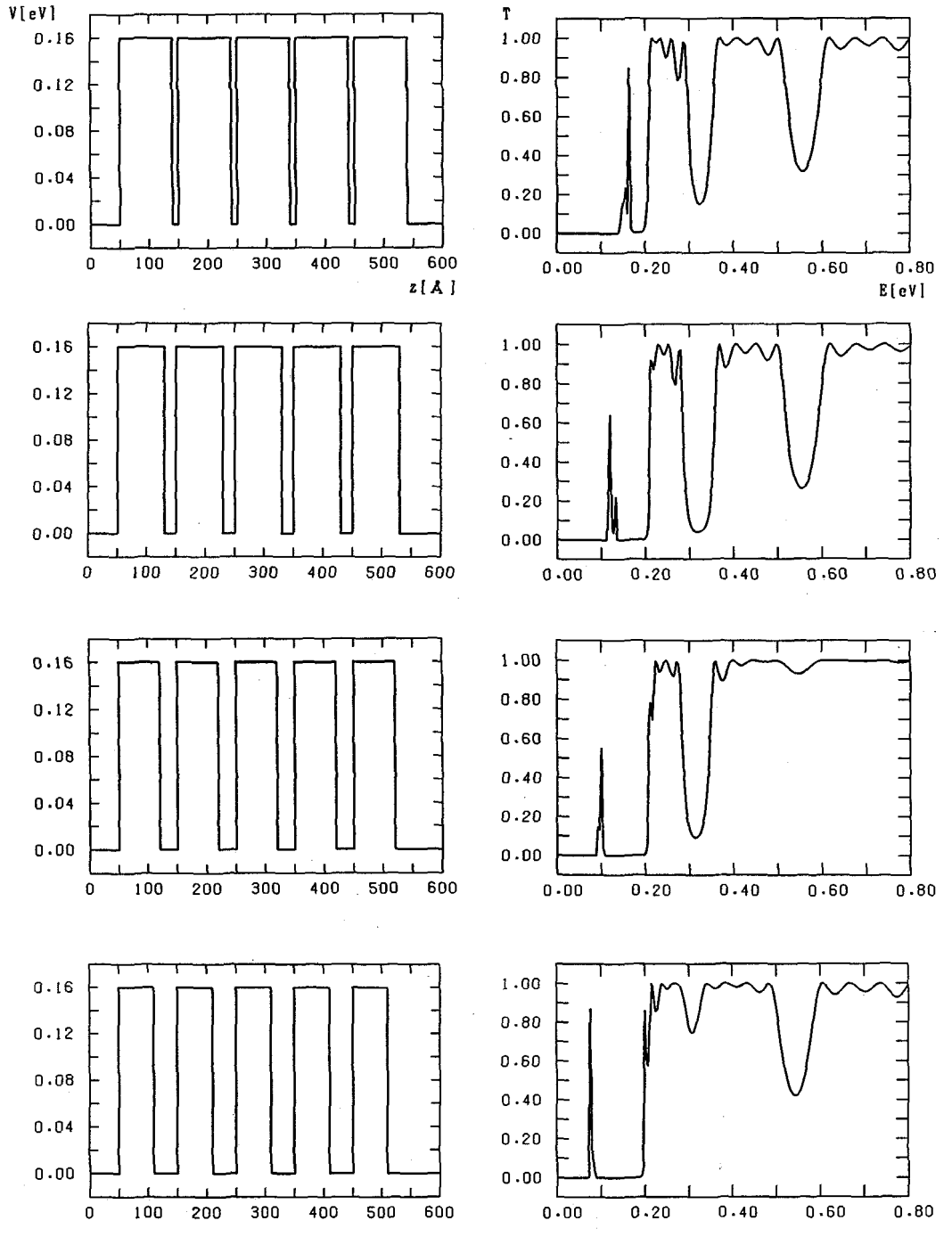

Fig.4a. Characteristics of arrays of potential steps. The ratio of the widths of valleys and barriers is systematically changed from 1:9 to 9:1.

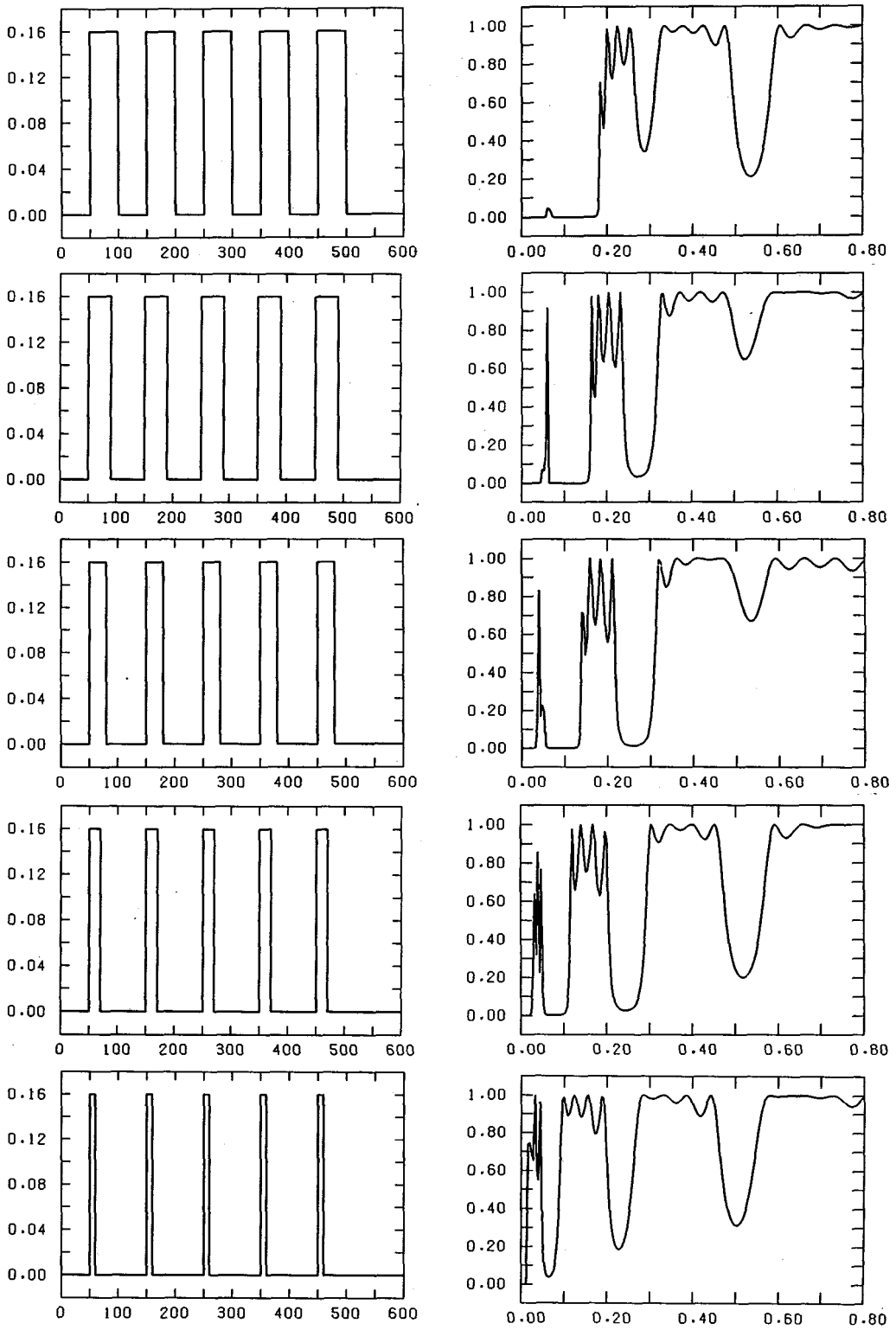

Fig.4a. (continued)

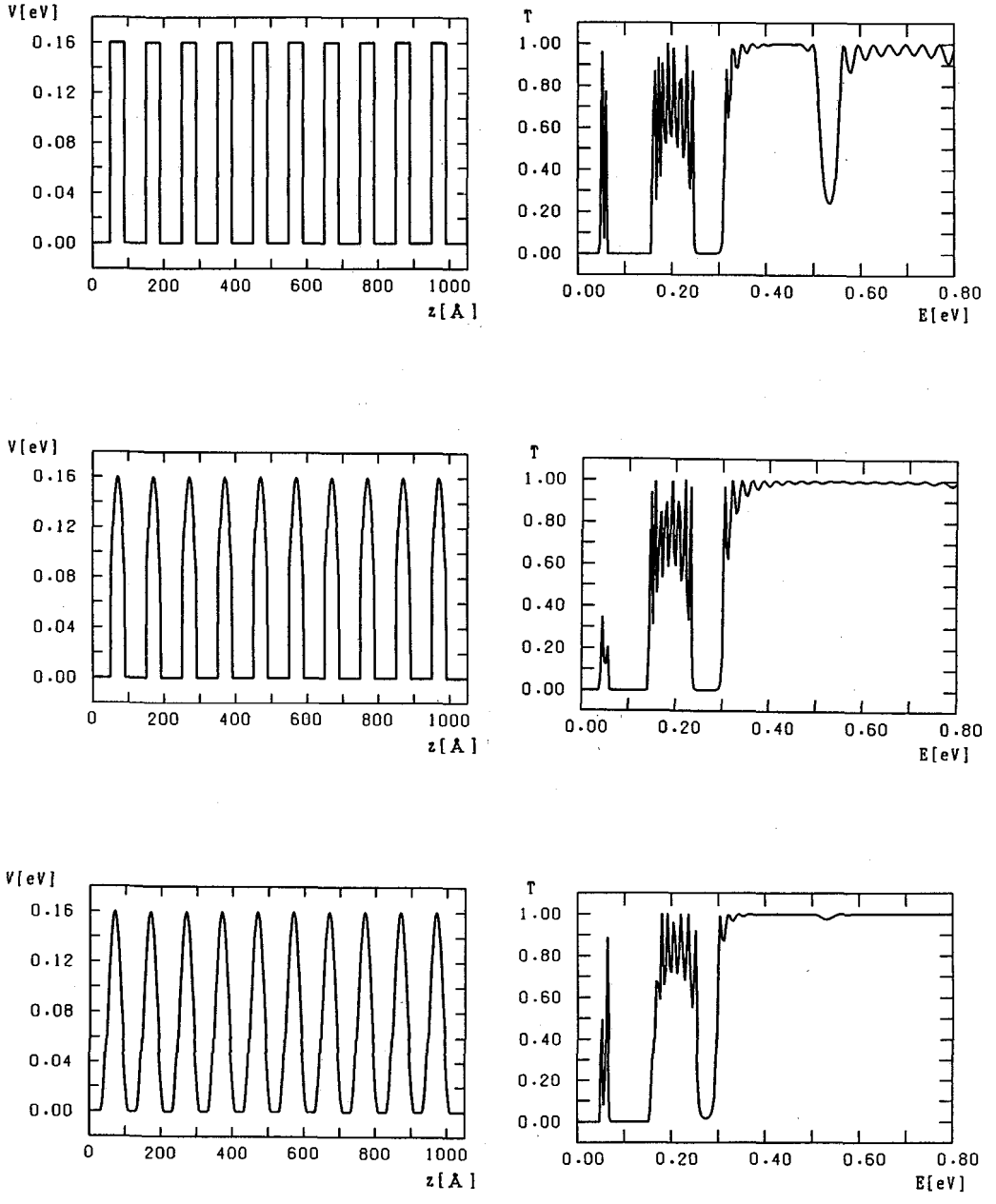

Fig.4b. Effect of details of potential profile in comparison with the case of square potential steps with valley-barrier ratio 6:4 shown at the top.

(c) Effect of fluctuation of potential structure

The potential profiles of fabricated superlattices are naturally subject to fluctuations coming from various origins. The effect of these fluctuations may be analyzed by changing randomly the thickness, the position, and the height of the barriers. Since the randomness in the third is in a sense redundant with those in the first and second and the concentration of Al can be controlled continuously, we here consider only the fluctuations in thicknesses and positions.

As a measure of the randomness, we take 3Å or the thickness of monolayer of these semiconductor lattices. The results of random fluctuations in the potential profile with the characteristics plotted in Figs.5a and 5b are shown in Figs.5c and 5d where several results of random changes are plotted in the same figure: In Figs.5c and 5d, the thickness and both the thickness and the position of barriers are randomly changed, respectively.

We observe that the forbidden bands are affected only slightly by fluctuations. The efficiency of allowed bands, however, decreases. This tendency is most remarkable for the lowest band as shown in enlarged scale in Figs.5b-5d.

4. Conclusion

The propagation of carriers through semiconductor superlattice potentials has been analyzed based on the solution of the Schrödinger equation by the finite element method.

The effects of linear and smooth gradings of the potential barriers are analyzed and it has been shown that the smooth grading is effective in reducing the oscillations of the transmission coefficient and almost classical transmission is obtained by the barrier with such gradings at both ends.

In the case of arrays of barriers which work as energy filters, the characteristics are obtained systematically for different ratios between the well width and barrier thickness. The results indicate that it is rather difficult to predict the properties of these filters without numerical computations such as the ones performed in this paper.

The effects of random fluctuation of structures on propagation properties have also been analyzed and are shown to appear mainly as a reduction of effectiveness in allowed bands.

In these investigations, this kind of numerical approach has been

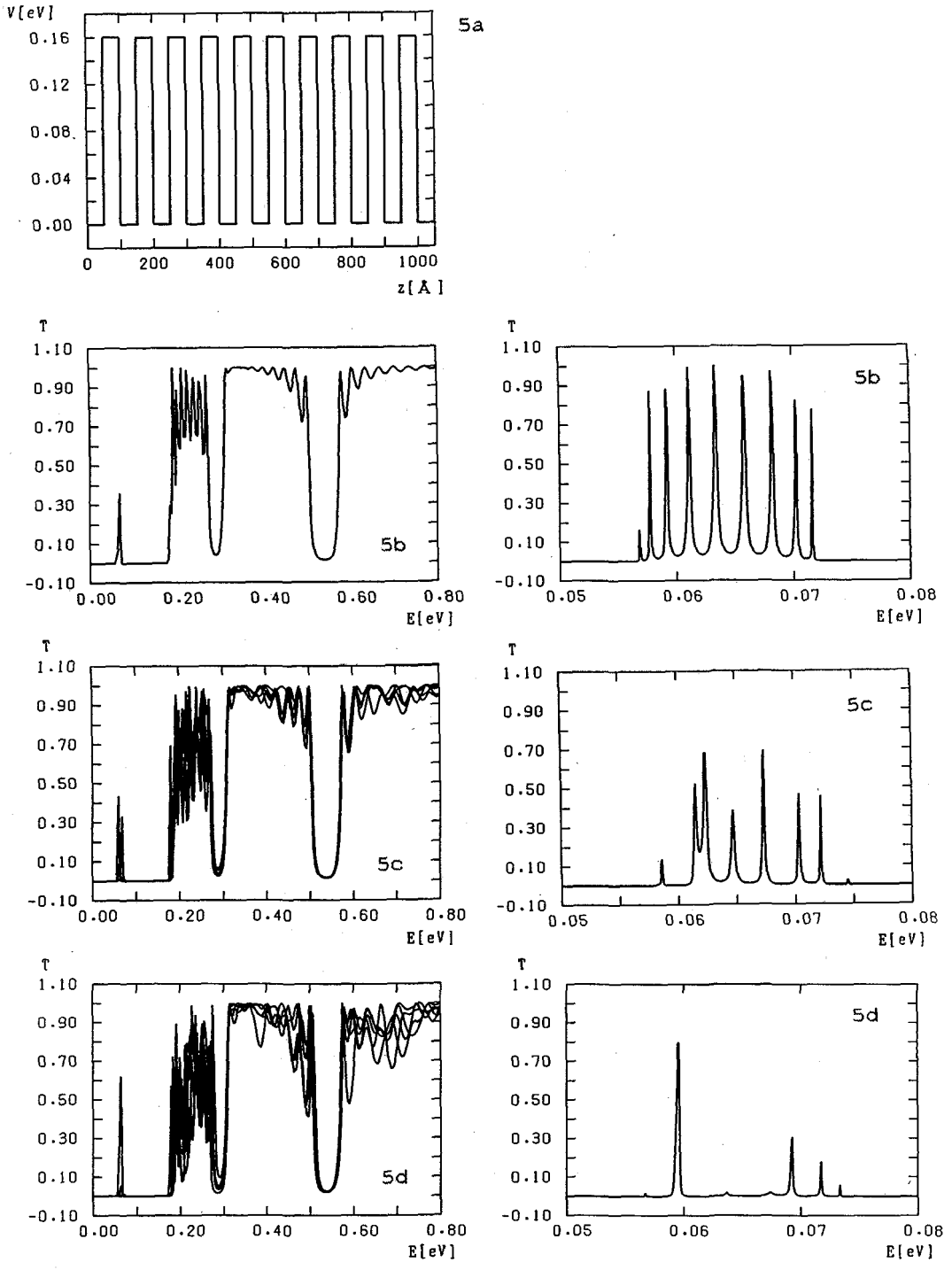

Fig.5a-5d. Effect of fluctuations in comparison with the case without fluctuation (a and b). Fluctuations in the width (c) and in both widths and positions (d) of barriers.

useful and we expect the usefulness will increase when we treat the cases with more complexity. One of such cases may be the two- and three-dimensional propagations and extensions in those directions are in progress.

Acknowledgments

The programs of the finite element method have been coded by H. Nakayama, S. Ishikura, and the authors. The authors thank them also for their collaboration in the early stages of this work. Numerical computations have been done at the Okayama University Computer Center.

References

1. L. Esaki and R. Tsu, IBM J. Res. and Dev. **14**, 61(1970).
2. F. Capasso and R. A. Kief, J. Appl. Phys. **58**, 1366(1985).
3. N. Yokoyama, K. Imamura, S. Muto, S. Hiyamizu, and H. Nishi, Japan. J. Appl. Phys. **24**, L853(1985).
4. T. K. Gaylord and K. F. Brennan, Appl. Phys. Lett. **53**, 2047(1988).
5. T. Ando and S. Mori, Surf. Sci. **113**, 124(1982).
6. For example, H. Kroemer, Surf. Sci. **174**, 299(1986).
7. For example, W. W. Lui and M. Fukuma, J. Appl. Phys., **60**, 1555(1986).
8. For example, K. Nakamura, A. Shimizu, M. Koshiba, and K. Hataya, Trans. of IEICE of Japan, **J71-C**, 1536(1988) (in Japanese).